***The Journal of Immunology* (10-03116-FL revised)**

GroEL1, a Heat Shock Protein 60 of *Chlamydia pneumoniae*, Induces Lectin-Like Oxidized Low-Density Lipoprotein Receptor 1 Expression in Endothelial Cells and Enhances Atherogenesis in Hypercholesterolemic Rabbits

Feng-Yen Lin[1,4,7], Yi-Wen Lin[1,7], Chun-Yao Huang[1,4,7], Yu-Jia Chang[6], Nai-Wen Tsao[2], Nen-Chung Chang[1,4], Keng-Liang Ou[7], Ta-Liang Chen[3,5], Chun-Ming Shih[1,4,*], Yung-Hsiang Chen[8,*]

[1]Division of Cardiology, [2]Division of Cardiovascular Surgery, and [3]Department of Anesthesiology, Taipei Medical University Hospital; [4]Department of Internal Medicine, [5]Department of Anesthesiology, School of Medicine, College of Medicine, [6]Graduate Institute of Clinical Medicine, [7]Research Center For Biomedical Implants and Microsurgery Devices, Taipei Medical University, Taipei; [8]Graduate Institute of Integrated Medicine, China Medical University, Taichung, Taiwan.

This work was supported by National Science Council (NSC 97-2314-B-038-035-MY2 and 99-2314-B-038-030-MY2), Taiwan.

* Address correspondence and reprint requests to Dr. Yung-Hsiang Chen and Dr. Chun-Ming Shih, Department of Internal Medicine, Taipei Medical University, No.250 Wu-Hsing St., Taipei, Taiwan. E-mail address: yhchen@mail.cmu.edu.tw and cmshih53@tmu.edu.tw

Ta-Liang Chen and Yung-Hsiang Chen contributed equally to this study.

Abbreviations used in this paper: *C. pneumoniae, Chlamydia pneumoniae*; LOX-1, lectin-like oxidized low-density lipoprotein receptor 1; HCAEC, human coronary artery endothelial cell; NADPH, nicotinamide adenine dinucleotide phosphate-oxidase; ROS, reactive oxygen species; MAPK, mitogen-activated protein kinase; TNF-α, tumor necrosis factor alpha; ESR, Erythrocyte sedimentation rate; CRP, C-reactive protein.

Running title: *C. pneumoniae* GroEL1 Induces LOX-1

Abstract

Lectin-like oxidized low-density lipoprotein (oxLDL) receptor 1 (LOX-1) plays a major role in oxLDL-induced vascular inflammation. *Chlamydia pneumoniae* has been found in atherosclerotic lesions and is related to atherosclerotic pathogenesis, although its specific mechanism remains unknown. This study was conducted to investigate the mechanisms of LOX-1 expression in GroEL1 (a heat shock protein from *C. pneumoniae*)-administered human coronary artery endothelial cells (HCAECs) and atherogenesis in hypercholesterolemic rabbits. We demonstrated that in the hypercholesterolemic rabbit model, GroEL1 administration enhanced fatty streak and macrophage infiltration in atherosclerotic lesions, which may be mediated by elevated LOX-1 expression. In vitro study using HCAECs, stimulation with GroEL1 increased TLR4 and LOX-1 expression. Increased LOX-1 expression was downregulated by Akt activation and PI3K-mediated eNOS activation. PI3K inhibitor and NOS inhibitor induced LOX-1 mRNA production, while the NO donor ameliorated the increasing effect of LOX-1 mRNA in GroEL1-stimulated HCAECs. LOX-1 expression was regulated by NADPH oxidase, which mediates ROS production and intracellular mitogen-activated protein kinase signaling pathway in GroEL1-stimulated HCAECs. Treatment with polyethylene-glycol-conjugated SOD, apocynin, or DPI significantly decreased GroEL1-induced LOX-1 expression, as did the knockdown of Rac1 gene expression by RNA interference. In conclusion, The GroEL1 protein may induce LOX-1 expression in endothelial cells and atherogenesis in hypercholesterolemic rabbits. The elevated level of LOX-1 *in vitro* may be mediated by the PI3K/Akt signaling pathway, eNOS activation, NADPH oxidase-mediated ROS production, and MAPKs activation in GroEL1-stimulated HCAECs. The GroEL1 protein of *C. pneumoniae* may contribute to vascular inflammation and cardiovascular disorders.

Keywords: atherosclerosis; *Chlamydia pneumoniae*; GroEL1; inflammation; LOX-1

Introduction

Chlamydia pneumoniae is a Gram-negative bacterium that has a biphasic elementary body and reticulate body life cycle. There is extensive evidence indicating that *C. pneumoniae* may play a key role in the development of atherosclerosis and coronary artery disease (1) Clinical evidence has shown that early fatty streaks present accumulation of *C. pneumoniae,* and seropositivity is associated with increasing vascular intima-media thickness (2). Inoculation of *C. pneumoniae* in animals may induce the formation of atherosclerotic lesions in hypercholesterolemic conditions (3). However, another study demonstrated that *C. pneumoniae* accelerates the formation of complex atherosclerosis in ApoE3-Leiden mice (4) and can induce increased uptake of low density lipoprotein (LDL) in macrophages (5). Although *C. pneumoniae* can induce LDL oxidation within the neointima (6) and may potentially increase the development of hypercholesterolemia-mediated atherosclerosis, there is no direct evidence of *C. pneumoniae* infection preceding oxidized LDL (oxLDL)-mediated atherogenesis.

During the infectious process of *C. pneumoniae* in target cells, elementary bodies (EBs) require both attachment to and phagocytosis by host cells (7). Heat shock protein 60 of *C. pneumoniae* (GroEL) is also expressed on the surface of EBs and the proteins could be fallen off from the EBs. Reports have demonstrated that the EB surface-associated GroEL1 is the major binding adhesion protein and plays an important role in the pathogenesis of infectious diseases (8). In clinical practice, the GroEL1 protein indeed causes several complicated diseases, including respiratory tract diseases and vascular diseases (9). Additionally, the GroEL1 protein may initiate the secretion of interleukin (IL)-6 and tumor necrosis factor (TNF)-α in dendritic cells, and stimulate production of IL-1β, -6, and -8 and proliferation in vascular cells and

mononuclear cells by triggering intracellular signaling pathway activation within eukaryotic cells (10-12).

One crucial event for *C. pneumonia*-induced atherosclerosis in believed to be oxLDL accumulation, which results in the formation of foam cells. Even though *C. pneumonia* infection enhances LOX-1 but not SREC (scavenger receptor expressed by endothelial cell) expression (13), which accelerates atherogenesis in the presence of hypercholesterolemia. We hypothesized that *C. pneumoniae* GroEL1 protein may increase LOX-1 expression in the endothelium, which mediates oxLDL uptake and the development of serious atherosclerosis. Therefore, we also examined whether GroEL1 increased neointimal hyperplasia and LOX-1 expression in hypercholesterolemic rabbits. Furthermore, we explored the cellular events and underlying mechanisms involved in GroEL1-induced LOX-1 expression using human coronary artery endothelial cells (HCAECs) *in vitro*.

Materials and Methods

Production and Purification of Chlamydia Pneumonia Elementary Bodies

Chlamydia pneumonia (*C. pneumonia*; TWAR TW-183) were cultured on Hela 229 cells, and 100 mL of inoculum from –70°C storage was used in Heppes/Sucrose/ Citrate dilution. Plates were centrifuged 1 h at 70g to enhance cellular attachment. The supernatant was aspirated and discarded, and Chlamydial Growth Media was added. Plates were incubated at 36 °C with CO_2 for 3 days, and then infected cells were harvested. The harvested cells were sonicated for 15 seconds, then centrifugated at 700 g for 15 min, then pelleted at 18,000 g at 4 °C for 30 min. The pellet was resuspended in HSC solution. The 3-5 mL of suspension was layered over a 13 mL HSC adding 7 mL Renografin and centrifuged 18,000 g at 4 °C for 30 min. The final suspension containing elementary bodies were to the original volume in 0.01 M PBS.

Construction of C. pneumoniae GroEL expression vectors

The genomic DNA of *C. pneumonia* was extraction from elementary bodies using EasyPure Genomic DNA mini kit (Bioman Scientific Co., Taipei, Taiwan). Segment containing the open-reading frame of the GroEL was originally PCR amplified by using 100 ng *C. pneumonia* genomic DNA as template, 0.2 mM dNTPs, 1 μM each of gene specific primers and 1 U Pfu DNA polymerase (Promega, Madison, WI, USA) with the following program: one cycle of 95°C for 5 min; 38 cycles of 95 °C for 45 sec, 68°C for 45 sec, and 72 °C for 2 min; and 1 cycle of 68 °C for 45 sec and 72 °C for 10 min; and a final incubation at 72 °C for 10 min with 1 U Taq DNA polymerase. The following gene specific primers were used in the PCR reaction: GroEL Pr-forward: 5’-CGAATTCTTAAGGAGAACAACGATGGCAG-3’ (forward primers contained an EcoRI site) and GroEL Pr-reverse:

5’-ACGGCCGGTAGTCCATTCCTGCGCTTGG C-3’ (reverse primers contained an EagI site). The amplified GroEL cDNA fragment was then cloned into pCR2.1-TOPO vector (Invitrogen, Carlsbad,CA,USA), and subsequently cloned in-frame into the EcoRI and NotI sites of pGEX-5X-1 expression vector (GE Healthcare Amersham Biosciences, USA) for expression in *E. coli*.

Purification of GroEL recombinant protein

BL21 cells were transformed with pGEX-5X-1-GroEL expression vector and GroEL recombinant proteins were purified. Briefly, the BL21 cells containing pGEX-5X-1-GroEL plasmid were grown overnight at 37 °C in 2 mL LB medium supplemented with 100 μg/ mL ampicillin. Then 1.25 mL of overnight culture was transferred into 100 mL LB/ampicillin medium and grown at 37 °C to an A600 of 0.6-0.8 (about 2 h). Fusion protein expression was then induced by adding IPTG to a final concentration of 1 mM at 30 °C for 6 h. Bacteria were pelleted by centrifugation for 10 min at 8000 rpm and recombinant GroEL was extracted under native conditions according to the protocol of GST Gene Fusion System manufacturer’s instructions (GE Healthcare Amersham Biosciences, USA). Finally, recombinant GroEL protein was purified by elution buffer containing 50 mM Tris-HCl and 10 mM reduced glutathione (pH 8.0). The quantity of recombinant GroEL protein was measured using the Bio-Rad Protein Assay (Bio-Rad, Hercules, CA, USA). The fusion protein were detected by SDS gel electrophoresis, and identified by immunoblotting with a GST antibody (GE Healthcare Amersham Biosciences, USA). Endotoxin levels in the recombinant GroEL protein were measured using a Limulus Amebocyte Lysate kit from Cambrex Inc. in USA. LPS levels were below 1 pg/mL.

Measurement of GroEL1 protein cytotoxicity and activity

Cell cytotoxicity of recombinant GroEL protein was analyzed by the 3-(4,5-dimethylthiazol-2-yl)-2,5-diphenyl tetrazolium bromide (MTT) assay. Human coronary artery endothelial cells (HCAECs) were grown in 96-well plates and incubated with various concentrations (1-500 ng/ml) of recombinant GroEL for 24 h. Subsequently, 0.5 μg/ml of MTT was added to each well, and incubation was continued at 37°C for an additional 4 h. Dimethyl sulfoxide was added to each well, and the absorbance was recorded at 530 nm using a DIAS Microplate Reader (Dynex Technologies, VA, USA). The activity of recombinant GroEL was measured by Enzyme-linked immunosorbent assay (ELISA). Human monocytic cell line, THP-1 cells, were seeded in 24-well plates at a density of 10^6 cells/ml/well, and these were then treated with various concentrations of GroEL protein (1-100 ng/ml) for 1 or 3 h. The culture medium was collected to quantify the levels of tumor necrosis factor alpha (TNF-α) using the DuoSet ELISA development kits (R&D Biosystems, CA, USA), and the absorbance was recorded using a DIAS Microplate Reader (Dynex Technologies, VA, USA).

Animal experiment

All animals were treated according to protocols approved by the Institutional Animal Care Committee of the Taipei Medical University (Taiwan). Experimental procedures and animal care conformed to the ‘‘Guide for the Care and Use of Laboratory Animals’’ published by the US National Institutes of Health (NIH Publication No. 85-23, revised 1996). Fifteen adult male New Zealand white rabbits (2.5–3 kg) were used. After 1 week on a commercial rabbit chow diet (Scientific Diet Services, Essex, UK) at 60 g/kg per day with water *ad libitum*, 9 animals were placed

on a 2% high-cholesterol (HC) diet (Purina Mills Inc., St. Louis, MO, USA) and 6 animals placed on a normal diet. The animals were divided into 5 groups: group 1 was the control; group 2 received the HC diet; group 3 received the HC diet and intravenous injections of GroEL1 (2 μg/kg body weight) through the ear vein at the end of weeks 2, 3, and 4; group 4 received the HC diet and intravenous injections of GroEL1 (4 μg/kg body weight) at the end of weeks 2, 3, and 4; and group 5 received the normal chow diet and GroEL1 (4 μg/kg body weight) at the end of weeks 2, 3, and 4. The animals were sacrificed and the abdominal aortas were then harvested, gently dissected free of adherent tissues, rinsed with ice-cold phosphate buffered saline (PBS), immersion-fixed with 4% buffered paraformaldehyde, paraffin-embedded, and then cross-sectioned for morphometry (hematoxylin and eosin staining) and immunohistochemistry. The thoracic aortas were also collected and stained with Sudan IV solution for visualization of the fatty streak areas.

Measurement of erythrocyte sedimentation rate (ESR) and serum C-reactive protein (CRP)

Erythrocyte sedimentation rate (ESR) and serum C-reactive protein (CRP) levels were analyzed to evaluate GroEL1-induced systemic inflammatory responses. Arterial blood was collected from the ear artery into tubes containing sodium citrate. ESR is used primarily to detect occult processes and monitor inflammatory conditions. Rabbit ESR was measured by the Westergren method. CRP is regarded as an acute phase reactant in the serum in a wide variety of diseases. Rabbit serum was separated from whole blood, and CRP was then measured in triplicate with a commercial ELISA kit (Immunology Consultants Laboratory, OR, USA).

Biochemical measurements

Blood samples for biochemical measurements were collected from each animal before and at 2 and 5 weeks of the experiment. Samples were separated by centrifugation and the serum was stored at −80°C until analysis. Serum total cholesterol and triglyceride were measured using Merck assay kits (Parmstadt, Germany). Serum blood urea nitrogen (BUN), creatinine, alanine aminotransferase (ALT), and aspartate aminotransferase (AST) were also measured using a SPOTCHEMTM automatic dry chemistry system (SP-4410; Arkray, Shanghai, Japan).

Sudan IV staining of arteries for fatty streaks

The fixed thoracic aortas were immersed in 70% ethanol for 30 min and then in the 1% Sudan IV/70% ethanol solution at room temperature for 2 h. The samples were then dipped in 70% ethanol for 3 minutes and rinsed with running tap water. Sudanophilic areas were measured quantitatively by computer-assisted planimetry and the extent of the lesions was expressed as a proportion of the total surface area (surface area of lesions/total surface area of the thoracic aorta).

Cell culture

HCAECs were purchased from Cascade Biologics, Inc. (Portland, OR, USA). Human monocytic THP-1 cells were purchased from American Type Culture Collection (Manassas, VA, USA). Cell cultures and passages were performed according to the manufacturer's instructions. HCAECs were used at passages 3–8. Purity of the HCAECs cultures was verified by immunostaining with a monoclonal antibody directed against smooth muscle-specific α-actin (R&D Systems,

Minneapolis, MN, USA).

Immunohistochemical and immunofluorescent staining

Immunohistochemical and immunofluorescent staining were performed on serial 5-μm-thick paraffin-embedded sections of rabbit abdominal aortas and cover slip-grown HCAECs using anti-LOX-1, anti-scavenger receptor expressed by endothelial cells (SREC), scavenger receptor B1 (SR-B1), or anti-RAM-11 antibodies. 2-(4-Amidinophenyl)-6-indolecarbamidine dihydrochloride (DAPI) was used to identify the nucleus. The slides were observed with microscopy or confocal microscopy.

Uptake of DiI-LDL by HCAECs

Human LDL (d:1.019-1.063 g/ml) was isolated by sequential ultracentrifugation of fasting plasma samples from healthy adult males (14). The native LDL was oxidized as described by Steinbrecher *et al* (15). Label the oxLDL with 1,1'-dioctadecyl-3,3,3',3'-tetramethyl-indocarbocyanine perchlorate (Dil) as described previously (16). To examine cellular uptake of oxLDL, HCAECs were seated on culture slides and incubated for 4 hours in cultured medium containing 80 μg/mL of Dil-labeled oxLDL. At the end of the treatment, cells were washed with PBS, mounted on cover slips, and examined with confocal microscopy.

Western blot analysis

Membrane fractions and total cell lysates were extracted from HCAECs. Proteins were separated by SDS–PAGE and transferred to PVDF membrane. The membranes were probed with mouse anti-LOX-1 (Santa Cruz Biotechnology, CA, USA),

anti-SREC (Santa Cruz Biotechnology, CA, USA), anti-SR-B1 (Santa Cruz Biotechnology, CA, USA), anti-eNOS (Millipore, MA, USA) anti-phospho-eNOS (Millopore, MA, USA), anti-Akt (Anaspec, CA, USA), anti-phospho-Akt (Merck, Darmstadt, Geremany), goat anti-TLR4 (R&D Systems, MN, USA), goat anti-TLR2 antibody (R&D Systems, MN, USA), rabbit anti-p38, rabbit anti-phospho-p38, rabbit anti-SAPK/JNK, rabbit anti-phospho-SAPK/JNK, rabbit anti-p44/p42 MAPK, or mouse anti-phospho-p44/p42 MAPK antibody (All MAPK antibodies were purchased from Cell Signaling Technology in USA). The proteins were visualized with an enhanced chemiluminescence (ECL) detection kit (Amersham Biosciences, NJ, USA). Mouse anti-α-actin (Labvision/NeoMarkers, CA, USA) and rabbit anti-Gαs (Santa Cruz Biotechnology, CA, USA) antibodies were used as loading controls.

Quantitative real-time polymerase chain reaction

Total RNA was isolated using TRIzol® Reagent (Invitrogen, Carlsbad, CA, USA) according to the manufacturer's instructions. LOX-1 and SREC mRNA expression were determinate using quantitative real-time polymerase chain reaction. The level of LOX-1 and SREC mRNA expression was determined in arbitrary units by comparison with an external DNA standard, which was amplified with the LOX-1 and SREC primers. PCR primers used for the amplification of LOX-1 and glyceraldehyde-3-phosphate dehydrogenase (GAPDH) mRNAs were:

LOX-1 forward primer: 5′-AAGGACCAGCCTGATGAGAA-3′
reverse primer: 5′-GCTGAGATCTGTCCCTCCAG-3′

SREC forward primer: 5′-CCTCAGCTCCCACAAGCTAC-3′
reverse primer: 5′-GAACCTCATCTGCCTCTCCA-3′

SR-B1 forward primer: 5′-CTGTGGGTGAGATCATGTGG-3′

reverse primer: 5′-GCCAGAAGTCAACCTTGCTC-3′

GAPDH forward primer: 5′-TGCCCCCTCTGCTGATGCC-3′

reverse primer: 5′-CCTCCGACGCCTGCTTCACCAC-3′

Knockdown gene expression with interference RNA

Intracellular TLR2 and TLR4 expression was knocked down by transfection with interference RNA (siRNA). Cells (10^6) were trypsinized and resuspended in 100 mL of Nucleofector solution (Amaxa Biosystems, Germany), and 30 nM of TLR2 or TLR4 siRNA (Ambion, TX, USA) were electroporated according to the manufacturer's instruction manual. The cells were seeded into six-well plates immediately after transfection or, for further experiments, after 48 h. Silencer validated siRNA (negative control siRNA, Ambion Catalog #4635, TX, USA) was used for knock-down validation.

NADPH oxidase activity assay

NADPH oxidase activity was determined with superoxide-dependent lucigenin chemiluminescence, as previously described(18). The 40 μg membrane protein extraction and 5 μM dark-adapted lucigenin were added to a 96-well luminometer plate and adjusted to afinal volume of 250 μL with oxidase assay buffer before 100 μM NADPH was added. Relative light units (RLU) were read with a luminometer (Dynatech ML2250, Dynatech Laboratories Inc., VA, USA). Light emission was recorded every minute for 15 min and was expressed as mean RLU/min.

Pull-down assay for Rac1 activity

Rac1 activation was measured using a glutathione S-transferase-(p21-activated

kinase)-p21 binding domain (GST-[PAK]-PBD) fusion protein, which binds to activated Rac1. HCAECs were lysed in lysis buffer (25 mM HEPES, 150 mM NaCl, 1% Igepal CA-630, 10% glycerol, 10 mM MgCl2, 1 mM EDTA, 10 μg/mL leupeptin, 10 μg/mL aprotinin). The supernatant was collected and incubated with GST-(PAK)-PBD fusion protein. The protein-bead complexes were then recovered by centrifugation and washed. Following the last wash, the protein-bead complexes were resuspended in SDS reducing sample buffer and resolved by 12% SDS-PAGE. The proteins were transferred to PVDF membrane and the membrane was incubated with mouse anti-Rac1 antibody (Upstate, IL, USA) and HRP-conjugated secondary antibody. Activated Rac1 was then detected using an ECL detection kit.

Statistical analyses

Values are expressed as means ± SEM. Statistical evaluation was performed using Student's *t*-test and one- or two-way ANOVA followed by Dunnett's test. A probability value of $P < 0.05$ was considered significant.

Results

High concentrations of GroEL1 induces THP-1 cell TNF-α production and HCAEC cytotoxicity

Treatment of HCAECs with 1, 10, 25, 50, 100, or 250 ng/mL of GroEL1 protein for 24 h did not result in cell viability (supplemental Fig. 1A). In contrast, a high concentration (500 ng/mL) of GroEL1 protein may cause a significant reduction in cell viability. Treatment of THP-1 cells with 100 ng/mL of GroEL1 for 1 h and 1–100 ng/mL of GroEL1 for 3 h may induce TNF-α production (supplemental Fig. 1B). The results indicated that recombinant GroEL1 has bio-activity and results in cell cytotoxicity at high concentrations.

Biochemical measurements for rabbits

During the experimental period, weight gain and final weight did not differ significantly between the groups of animals (data not shown). As shown in Table 1, serum AST, ALT, BUN, and creatinine levels also showed no significant difference between groups. Serum total cholesterol levels were increased after 2-week HC diet. At the end of the fifth experimental week, the HC diet may have the elevated total cholesterol level. Compared to the control group, GroEL1 protein treatment did not increase the serum total cholesterol level. Additionally, serum triglyceride levels did not increase significantly in any group during the experimental period.

GroEL1 protein induces inflammatory responses in rabbits

ESR and serum CRP levels were analyzed to monitor GroEL1-induced systemic inflammation (Table 2). In the control and HC diet groups, ESR and CRP levels did not change during the experiment. However, ESR increased in the GroEL1 groups at week 4 and week 5. CRP levels increased at week 3 and continued to increase

throughout the experimental period. During the experimental period, heart rate, rectal body temperature, and respiratory rate of the rabbits were monitored. This result suggests that GroEL1 protein injection may keep rabbits in a non-sepsis state and induce chronic combining acute systemic inflammation.

GroEL1 enhances atherosclerotic lesion formation in HC diet-fed rabbits

Representative photographs of the fatty streaks of thoracic aortas stained with Sudan IV from the 5 groups are shown in Fig. 1A. There were no atherosclerotic lesions in the aortas of control rabbits. Sudanophilic atherosclerotic lesions in the HC diet group were slightly increasing under *en face* observation. A significant area of the aortic intimal surface from the HC diet + 2 μg/kg BW GroEL1 group and the HC diet + 4 μg/kg BW GroEL1 group was covered with fatty streaks. Furthermore, use of 4 μg/kg BW GroEL1 induced more serious fatty streak formation than use of 2 μg/kg BW GroEL1 in rabbits fed an HC diet. In contrast, administration of 4 μg/kg BW GroEL1 protein did not increase atherosclerotic lesion formation in rabbits fed a normal chow diet.

Figure 1B shows that rabbits in the control, HC diet, and 4 μg/kg BW GroEL1 groups did not have thickened intima or atherosclerotic lesion formation in the abdominal aortas. Abdominal aortas had slight lesion formation in the HC diet + 2 μg/kg BW GroEL1 group and markedly lesion formation in the HC diet + 4 μg/kg BW GroEL1 group compared with these areas in the control group. Staining with anti-RAM-11 antibody for identification of infiltrated macrophages showed that fewer macrophages infiltrated into the vessel walls in the control, HC diet, and 4 μg/kg BW GroEL1 groups compared to the HC diet + GroEL1 groups (Fig. 1C). These results demonstrate that administration of GroEL1 protein significantly increased

macrophage infiltration and atherosclerotic plaque formation in HC diet-fed rabbits.

LOX-1 expression in GroEL1-administered rabbits

Immunohistochemical staining was performed using antibodies against LOX-1, SREC and SR-B1 on sections of the abdominal aortas (Fig. 1D). Compared with sections from the control group, GroEL1 administration slightly enhanced LOX-1 expression in the endothelium of the HC diet group, while strong LOX-1 staining was seen on the luminal surface of the 4 μg/kg BW GroEL1 group and in the neointima of the HC diet + 4 μg/kg BW GroEL1 group. In contrast, neither HC diet nor GroEL1 administration induced SREC and SR-B1 expression in the abdominal aorta in rabbits. These results demonstrate that GroEL1 administration increased LOX-1 expression and significantly severed atherosclerotic lesion formation in the aorta.

GroEL1 induces LOX-1 expression and enhances DiI-oxLDL uptake in HCAECs

A DiI-oxLDL uptake assay was performed to investigate whether oxLDL uptake is enhanced in GroEL1-stimulated endothelial cells. Confocal microscopy demonstrated that treatment with GroEL1 protein for 24 h significantly increased DiI-oxLDL uptake in HCAECs (Fig. 2A). Real-time PCR demonstrated that GroEL1 treatment for 12 h may induce LOX-1 mRNA expression but not SREC or SR-B1 mRNA expression (Fig. 2B). Immunofluorescence also showed that treatment with GroEL1 protein for 24 h induces LOX-1 protein expression in HCAECs (Fig. 2C). LOX-1, SREC and SR-B1 were originally identified on the membrane of vascular endothelial cells; Western blotting showed that GroEL1 protein increases intracellular LOX-1 production and elevates membrane LOX-1 expression in HCAECs (Fig. 2D).

TLR4 mediates LOX-1 expression in GroEL1-stimulated HCAECs

C. pneumonia GroEL1 may induce innate immune responses *in vitro* via TLR2 and TLR4 (19). As shown in Figure 3A, GroEL1 protein significantly induced TLR4 expression but not TLR2 expression. Treatment with 100 ng/mL of GroEL1 for 12 h significantly induced LOX-1 mRNA expression (Fig.s 3B and 3C). Addition of a mouse anti-hTLR4 antibody (10 μg/mL) and subsequent incubation for 30 min or transfection with 25 nM TLR4 siRNA prior to GroEL1 treatment significantly reduced LOX-1 mRNA production in HCAECs. As a negative control in the competition assay, a nonspecific IgG2α isotype antibody was substituted for the TLR4-specific antibody; however, the nonspecific antibody and the silencer validated siRNA did not affect GroEL1-induced LOX-1 mRNA production (data not shown). In contrast, Figure 3C shows that mouse anti-hTLR2 antibody and TLR2 siRNA did not block LOX-1 mRNA production in GroEL1-stimulated HCAECs suggesting the GroEL1-induced LOX-1 expression in HCAECs is mediated by TLR4.

Akt signaling pathway and eNOS activity may be involved in GroEL1-induced LOX-1 expression

We next investigated the effects of GroEL1 protein on Akt kinase signals and eNOS expression in HCAECs. After 6 h of incubation, Akt phosphorylation was significantly decreased in GroEL1 protein-cultured HCAECs (Fig. 4A). Furthermore, eNOS phosphorylation at $Ser^{1,177}$ was significantly decreased both in GroEL1 protein-stimulated and LY294002 (a PI3K inhibitor)-treated HCAECs compared with control conditions (Fig. 4B). The PI3K/Akt signaling pathway did not involve eNOS production in GroEL1-stimulated HCAECs (LY294002 treatment did not decrease eNOS production; Fig. 4B), the potential roles of mitogen-activated protein kinase

(MAPK)-related mechanisms were also examined. Pretreatment with SB203580 (p38 MAPK inhibitor), SP600125 (a JNK/SAPK inhibitor), or PD98059 (an MEK1 antagonist) for 1 h did not ameliorate the inhibitory effects of GroEL1 protein on eNOS phosphorylation (Fig. 4C). Interestingly, GroEL1-stimulated decreases in eNOS production were reduced by SB203580 but not by SP600125 or PD98059. This result probably indicated that GroEL1 protein influences eNOS production mediating by p38 MAPK. The potential roles of PI3K/Akt and eNOS in LOX-1 expression in GroEL1-stimulated HCAECs were then examined. Co-incubation with NO donor *S*-nitrosocysteine (SNOC) significantly ameliorated the increases in LOX-1 mRNA (Fig. 4D) and LOX-1 protein (Fig. 4E) on GroEL1-stimulated HCAECs. In contrast, incubation with NOS inhibitor L-N^g-nitro-L-arginine methyl ester (L-NAME) or PI3K inhibitor LY294002 significantly enhanced LOX-1 expression. These data indicate that GroEL1 protein may upregulate LOX-1 expression in endothelial cells by modulating PI3K/Akt-, eNOS-, and p38 MAPK-related mechanisms.

GroEL1-induced LOX-1 expression is mediated by Rac1 and NADPH oxidase activation and ROS generation

To determine whether GroEL1 protein induces NADPH oxidase activation in HCAECs, HCAECs were treated with 100 ng/mL GroEL1 protein for 0 (●), 60 (○), 90 (▲), or 120 (△) min and the membrane fraction was then assayed for NADPH oxidase activity. GroEL1 protein treatment resulted in a time-dependent increase in enzyme activity. Diphenylene iodonium (DPI; 100 μM) was used to determine NADPH oxidase activity (Fig. 5A), which is associated with Rac1 activation insofar as it has been reported to play important roles in NADPH oxidase activation (20). To further examine whether GroEL1-induced NADPH oxidase activation is accompanied

by increases in Rac1 activation, we measured activated Rac1 with a GST-(PAK)-PBD fusion protein pull-down assay. HCAECs were treated with 25–100 ng/mL of GroEL1 protein for 120 min. Total cell lysates were extracted and measured for Rac1 activity. GroEL1 treatment rapidly induced Rac1 activation in a dosage-dependent manner (Fig. 5B). To explore whether NADPH-mediated ROS are involved in GroEL1-induced LOX-1 expression, HCAECs were pretreated with various antioxidants or transfected with Rac1 siRNA prior to stimulation with GroEL1 protein. As shown in Figure 5C, GroEL1 or of H_2O_2 significantly induced LOX-1 mRNA expression, which was significantly blocked by pretreatment with polyethylene-glycol-conjugated superoxide dismutase (PEG-SOD, a permeable antioxidant enzyme), apocynin (a specific NADPH oxidase inhibitor), or DPI for 1 h. GroEL1-induced LOX-1 mRNA expression was completely blocked by Rac1 when an RNA silencing technique was used but not by the negative control siRNA. These results suggest that GroEL1-induced LOX-1 expression is mediated by an oxidative stress-related mechanism and that the NADPH oxidase subunit Rac1 plays a critical role in LOX-1 regulation.

Intracellular MAPK signaling in GroEL1-induced LOX-1 expression

GroEL1 protein markedly induced the phosphorylation of MAPKs, including p38 MAPK, ERK1/2, and SAPK/JNK (Fig. 5D), after exposure to 25–100 ng/mL of GroEL1 protein for 30 min. DPI significantly decreased SAPK/JNK activation in GroEL1-stimulated HCAECs but did not influence p38 MAPK or ERK1/2 activation (Fig. 5D), suggesting that NADPH–oxidase-derived ROS are involved in SAPK/JNK signaling pathway activation. Real-time PCR demonstrated that GroEL1-induced LOX-1 mRNA expression was reduced by SB203580 (a p38 MAPK inhibitor),

SP600125 (an SAPK/JNK inhibitor), or SB203580 + SP600125 but not by PD98059 (an MEK1 antagonist) (Fig. 5E). These results suggest that SAPK/JNK and p38 MAPK play more significant roles than ERK1/2 in the GroEL1-mediated LOX-1 mRNA expression transcriptional regulatory signaling pathway.

Discussion

In the present study, we demonstrated for the first time that *C. pneumoniae* GroEL1 protein may enhance LOX-1 expression in endothelium and mediate oxLDL uptake and atherosclerosis progression. In fact, GroEL1 increased neointimal hyperplasia and LOX-1 expression in hypercholesterolemic rabbits. Furthermore, our *in vitro* findings suggest that GroEL1 interacts with TLR4 and plays critical roles in oxLDL-uptake of endothelial cells, which results from elevated LOX-1 expression and is mediated by NADPH oxidase activation, PI3K/Akt-mediated eNOS activation, and the MAPK signaling pathways.

C. pneumonia infection and atherogenesis

The role of *C. pneumoniae* infection in the pathogenesis of atherosclerosis remains controversial (21-24). Meta-analyses of randomized clinical trials of antibiotic therapy for secondary prevention of coronary heart disease did not show any benefit (25, 26). There was also no effect of possible *C. pneumoniae* infection on serological markers. Although these results do not conclusively rule out a role of *C. pneumoniae* in the pathogenesis of atherosclerosis, they definitively do not support the use of antibiotics in the secondary prevention of coronary heart disease. Our data showed that *C. pneumoniae* GroEL1 protein alone did not induce fatty streak formation but did enhance the formation of atherosclerotic lesions in HC diet-fed rabbits, suggesting the potential role of *C. pneumoniae* heat shock proteins in atherosclerosis induction in the presence of hypercholesterolemia. This may provide a potential rationale for the dramatic failure of clinical trials using antibiotics for atherosclerosis.

Studies have shown associations between atherosclerosis and different pathogens,

and early investigations showed the presence of infectious pathogens in the whole arterial vessel tree (27). It is known that pathogens such as *C. pneumoniae* can induce macrophage foam cell formation (28), an effect that might be increased if an individual has been infected by multiple pathogens (5). TLR/MyD88 and liver X receptor signaling pathways reciprocally control *C. pneumoniae*-induced acceleration of atherosclerosis (29). It has been hypothesized that the infectious pathogen contains proteins that are homologous to parts of the host proteins, resulting in an immune response called infection-induced molecular mimicry (30). It has recently been shown that *C. pneumoniae* heat shock protein 60 localizes in human atheroma and regulates macrophage TNF-α and matrix metalloproteinase expression (31); in fact, this heat shock protein 60 can activate human vascular endothelium, smooth muscle cells, and macrophages (10) and can stimulate cellular LDL oxidation *in vitro* (6). Our data show that administration of GroEL1 protein significantly increased macrophage infiltration in atherosclerotic plaques in HC diet-fed rabbits, supporting the results that genital chlamydia infections are associated with significant induction of the chemokines and chemokine receptors that are involved in the recruitment of immune cells into infection sites (32).

The hypercholesterolemic with GroEL1 administration rabbit model was used in the present study. Rabbits were injected with 2 or 4 μg/kg body weight GroEL1, which represents a GroEL1 level of 50 or 100 ng/mL of plasma, respectively. The combined results of ESR and serum CRP measurements are a useful indicator of inflammation. The rectal body temperature and respiratory rate of the rabbits were kept in the normal range (the normal range of rectal body temperature: 38-40℃ and respiratory rate: 30-60 breaths/min) after GroEL1 was administered. Elevated CRP and ESR, but the maintenance of normal vital signs, indicated that the dose of

GroEL1 was sufficient to produce inflammation in the animals, which remained in a nonseptic state. Indeed, we decided the dose of GroEL1 in the *in vivo* study with 25-100 ngmL was consistent with the pathophysiological state of hypercholesterolemic and GroEL1-administrated rabbit study, *in vivo*. Previous findings have demonstrated that a repertoire of LOX-1 is associated with atherosclerotic lesions. Although atherosclerotic plaques lipids can be found in macrophages and foam cells, and LOX-1 is not only expressed by endothelial cells, but also by smooth muscle cells and macrophages; therefore, we cannot be excluded that macrophages/smooth muscle cells via the GroEL1/LOX-1 route play some roles during atherogenesis. Further studies are required to clarify the interaction between GroEL1 and LOX-1 expression in smooth muscles and monocytes.

C. pneumonia and LOX-1 expression

The histopathological features of *C. pneumoniae*-induced aortic lesions closely resemble early changes produced by a diet enriched with low amounts (0.15%) of cholesterol in rabbits, which resulted in serum cholesterol levels (4.1 mM) similar to what is recommended for humans (33). *C. pneumoniae* infection was also found to accelerate the development of atherosclerosis in rabbits fed a cholesterol-enriched diet (34). Our data inconsistent with previous studies in which *C. pneumoniae* was detected in the atherosclerotic aorta in cholesterol-fed or apolipoprotein E (Apo-E)-deficient mice but did not induce vascular changes by itself (35); in mice with LDL receptor and Apo-E deficiencies, *C. pneumoniae* was found to exacerbate hypercholesterolemia-induced atherosclerosis (36, 37).

LOX-1 is a scavenger receptor that functions as the primary oxLDL receptor in endothelial cells and is implicated in oxLDL-induced endothelial dysfunction and

atherosclerosis. Recently, much emphasis has been placed on ox-LDL as a major mediator of endothelial activation and/or dysfunction. Specific ox-LDL receptors including LOX-1 and scavenger receptors have been described in endothelial cells, macrophages, and smooth muscle cells. These receptors facilitate uptake of ox-LDL and subsequent endothelial activation, transformation of macrophages to foam cells, and smooth muscle cell proliferation (38, 39). In the present study, we demonstrated that GroEL1 upregulates LOX-1 expression in HCAECs. Since LOX-1 is the main receptor for oxLDL and may play an important role in the pathogenesis of atherosclerosis, identification and regulation of LOX-1 and understanding its signal transduction pathways might improve our insight of the pathogenesis of atherosclerosis and provide a selective treatment approach. LOX-1 might be a potential and promising target for the development of novel anti-atherosclerotic drugs.

In the present study, exogenous addition of recombinant GroEL1 induced oxLDL uptake and LOX-1 expression in endothelial cells. TLR4 was the mediator in GroEL1-induced LOX-1 expression. These results suggest that the GroEL1-induced expression of LOX-1 in HCAECs is mediated by TLR4. This result is inconsistent with the observation that the mitogenic effect of *C. pneumoniae* on vascular smooth muscle cells could be mimicked by exogenous chlamydia HSP60 via a TLR4-mediated signaling pathway (12). Several groups have reported that TLR4 expression is upregulated by bacterial lipopolysaccharide and certain cytokines in endothelial cells (40), extracellular HSP60 may still act as a signal transducer to stimulate cells via upregulated TLR4.

Regulation of LOX-1

Induced endothelial expression of LOX-1 upon various pathologic stimuli would

provide a molecular link for incorporation of oxLDL into cells, resulting in cellular activation, dysfunction, and injury (41). Since oxLDL has been shown to generate ROS, tethering oxLDL via LOX-1 would focus oxidant stress on cellular targets, resulting in changes in gene expression and cellular phenotype and, in some cases, induction of endothelial dysfunction. Recent studies showed that oxLDL binding to LOX-1 in endothelial cells induces generation of superoxide anion (42). As DPI, a selective inhibitor of NADPH oxidase, drastically reduced intracellular superoxide concentration, oxLDL-induced superoxide generation might be related to increased NADPH oxidase activity. The increased intracellular superoxide anion accelerates NO inactivation (43). The presence of oxLDL decreases intracellular NO concentrations in basal, bradykinin-stimulated, and thrombin-stimulated conditions. In addition, in HCAECs, oxLDL decreases PKB/Akt phosphorylation and downregulates eNOS activity (44). Our data also demonstrated that GroEL1 induced LOX-1 expression in the Akt/eNOS-related pathway, which suggests that the Akt/eNOS-related pathway plays an important role in GroEL1-induced LOX-1 activation.

Production of oxLDL promotes free radical generation and causes lipid peroxidation in endothelial cells (45). LOX-1 activation is associated with intracellular free radical generation, which has a positive effect on LOX-1 expression (42). Regulation of LOX-1 gene expression is redox sensitive (46); therefore, ROS generated by GroEL1 in vascular cells may be key intermediates in the regulation of LOX-1 gene expression. Evidence linking oxidative stress with MAPK activation in vascular cells additionally supports a role of these kinases in the control of LOX-1 expression (47). In line with these hypotheses, we found that antioxidants and NADPH oxidase/MAPK inhibitors reduced GroEL1-induced LOX-1 levels, thus implicating ROS and kinases as signaling molecules in this effect. Our findings that

antioxidants suppressed GroEL1-induced NADPH oxidase/MAPK activation and that NADPH oxidase inhibition abolished GroEL1-induced MAPK activation support the hypothesis that GroEL1-induced kinase activation involves oxidative stress and that MAPKs act in this signaling cascade as intermediate molecules that carry signals from NADPH oxidase to endothelial LOX-1.

In this study, we had noted the preferred target of the various inhibitors/antagonists that were used in cellular analyses. We had performed the pilot study for the possible cytotoxicity amount these various kinase and oxidase inhibitors with MTT assay. No apparent cytotoxicity was found for the dosages that used in the study. Actually, the various kinase and oxidase inhibitors that using in this study can often have off target effects in various cell lines and types. In the further, we should have more direct evidences to verify the influence of GroEL1 on LOX-1 expression in HCAECs.

In conclusion, our results demonstrated that the *C. pneumoniae* GroEL1 protein may induce LOX-1 expression in endothelial cells, which mediates fatty streak formation in atherogenesis. The elevated level of LOX-1 may be mediated by the PI3K/Akt signaling pathway, eNOS activation, NADPH oxidase-mediated ROS production, and MAPKs activation in GroEL1-stimulated HCAECs. The *C. pneumoniae* GroEL1 protein may contribute to vascular inflammation and cardiovascular disorders. Our work identifying LOX-1 as a target gene for GroEL1 provides a basis for further investigation of LOX-1 modulation as a therapeutic strategy for atherogenesis in *C. pneumoniae* infection.

Acknowledgements

We also thank Tze-Liang Yang and Min-Yu Lo for excellent technical

assistance.

Disclosures

The authors have no financial conflicts of interest.

References

1. Xu, Q. 2003. Infections, heat shock proteins, and atherosclerosis. *Curr Opin Cardiol* 18:245-252.
2. Volanen, I., M. J. Jarvisalo, R. Vainionpaa, M. Arffman, K. Kallio, S. Angle, T. Ronnemaa, J. Viikari, J. Marniemi, O. T. Raitakari, and O. Simell. 2006. Increased aortic intima-media thickness in 11-year-old healthy children with persistent Chlamydia pneumoniae seropositivity. *Arterioscler Thromb Vasc Biol* 26:649-655.
3. Blessing, E., L. A. Campbell, M. E. Rosenfeld, N. Chough, and C. C. Kuo. 2001. Chlamydia pneumoniae infection accelerates hyperlipidemia induced atherosclerotic lesion development in C57BL/6J mice. *Atherosclerosis* 158:13-17.
4. Ezzahiri, R., H. J. Nelissen-Vrancken, H. A. Kurvers, F. R. Stassen, I. Vliegen, G. E. Grauls, M. M. van Pul, P. J. Kitslaar, and C. A. Bruggeman. 2002. Chlamydophila pneumoniae (Chlamydia pneumoniae) accelerates the formation of complex atherosclerotic lesions in Apo E3-Leiden mice. *Cardiovasc Res* 56:269-276.
5. Kalayoglu, M. V., and G. I. Byrne. 1998. Induction of macrophage foam cell formation by Chlamydia pneumoniae. *J Infect Dis* 177:725-729.
6. Kalayoglu, M. V., B. Hoerneman, D. LaVerda, S. G. Morrison, R. P. Morrison, and G. I. Byrne. 1999. Cellular oxidation of low-density lipoprotein by Chlamydia pneumoniae. *J Infect Dis* 180:780-790.
7. Hybiske, K., and R. S. Stephens. 2007. Mechanisms of host cell exit by the intracellular bacterium Chlamydia. *Proc Natl Acad Sci U S A* 104:11430-11435.
8. Zugel, U., and S. H. Kaufmann. 1999. Role of heat shock proteins in protection from and pathogenesis of infectious diseases. *Clin Microbiol Rev* 12:19-39.
9. Borel, N., J. T. Summersgill, S. Mukhopadhyay, R. D. Miller, J. A. Ramirez, and A. Pospischil. 2008. Evidence for persistent Chlamydia pneumoniae infection of human coronary atheromas. *Atherosclerosis* 199:154-161.
10. Kol, A., T. Bourcier, A. H. Lichtman, and P. Libby. 1999. Chlamydial and human heat shock protein 60s activate human vascular endothelium, smooth muscle cells, and macrophages. *J Clin Invest* 103:571-577.
11. Krull, M., A. C. Klucken, F. N. Wuppermann, O. Fuhrmann, C. Magerl, J. Seybold, S. Hippenstiel, J. H. Hegemann, C. A. Jantos, and N. Suttorp. 1999. Signal transduction pathways activated in endothelial cells following infection with Chlamydia pneumoniae. *J Immunol* 162:4834-4841.

12. Sasu, S., D. LaVerda, N. Qureshi, D. T. Golenbock, and D. Beasley. 2001. Chlamydia pneumoniae and chlamydial heat shock protein 60 stimulate proliferation of human vascular smooth muscle cells via toll-like receptor 4 and p44/p42 mitogen-activated protein kinase activation. *Circ Res* 89:244-250.
13. Yoshida, T., N. Koide, I. Mori, H. Ito, and T. Yokochi. 2006. Chlamydia pneumoniae infection enhances lectin-like oxidized low-density lipoprotein receptor (LOX-1) expression on human endothelial cells. *FEMS Microbiol Lett* 260:17-22.
14. Winocour, P. H., P. N. Durrington, D. Bhatnagar, M. Ishola, S. Arrol, and M. Mackness. 1992. Abnormalities of VLDL, IDL, and LDL characterize insulin-dependent diabetes mellitus. *Arterioscler Thromb* 12:920-928.
15. Steinbrecher, U. P., S. Parthasarathy, D. S. Leake, J. L. Witztum, and D. Steinberg. 1984. Modification of low density lipoprotein by endothelial cells involves lipid peroxidation and degradation of low density lipoprotein phospholipids. *Proceedings of the National Academy of Sciences of the United States of America* 81:3883-3887.
16. Oriol, A., J. M. Ribera, J. Arnal, F. Milla, M. Batlle, and E. Feliu. 1993. Saccharomyces cerevisiae septicemia in a patient with myelodysplastic syndrome. *American journal of hematology* 43:325-326.
17. Hatch, F. T. 1968. Practical methods for plasma lipoprotein analysis. *Adv Lipid Res* 6:1-68.
18. Smith, K. R., L. R. Klei, and A. Barchowsky. 2001. Arsenite stimulates plasma membrane NADPH oxidase in vascular endothelial cells. *American journal of physiology* 280:L442-449.
19. Costa, C. P., C. J. Kirschning, D. Busch, S. Durr, L. Jennen, U. Heinzmann, S. Prebeck, H. Wagner, and T. Miethke. 2002. Role of chlamydial heat shock protein 60 in the stimulation of innate immune cells by Chlamydia pneumoniae. *Eur J Immunol* 32:2460-2470.
20. Yokoyama, M., N. Inoue, and S. Kawashima. 2000. Role of the vascular NADH/NADPH oxidase system in atherosclerosis. *Ann N Y Acad Sci* 902:241-247; discussion 247-248.
21. Belland, R. J., S. P. Ouellette, J. Gieffers, and G. I. Byrne. 2004. Chlamydia pneumoniae and atherosclerosis. *Cell Microbiol* 6:117-127.
22. Grayston, J. T. 2000. Background and current knowledge of Chlamydia pneumoniae and atherosclerosis. *J Infect Dis* 181 Suppl 3:S402-410.
23. Ieven, M. M., and V. Y. Hoymans. 2005. Involvement of Chlamydia pneumoniae in atherosclerosis: more evidence for lack of evidence. *J Clin Microbiol* 43:19-24.

24. Kalayoglu, M. V., P. Libby, and G. I. Byrne. 2002. Chlamydia pneumoniae as an emerging risk factor in cardiovascular disease. *JAMA* 288:2724-2731.
25. Wells, B. J., A. G. Mainous, 3rd, and L. M. Dickerson. 2004. Antibiotics for the secondary prevention of ischemic heart disease: a meta-analysis of randomized controlled trials. *Arch Intern Med* 164:2156-2161.
26. Illoh, K. O., O. C. Illoh, H. B. Feseha, and J. M. Hallenbeck. 2005. Antibiotics for vascular diseases: a meta-analysis of randomized controlled trials. *Atherosclerosis* 179:403-412.
27. Saikku, P., M. Leinonen, L. Tenkanen, E. Linnanmaki, M. R. Ekman, V. Manninen, M. Manttari, M. H. Frick, and J. K. Huttunen. 1992. Chronic Chlamydia pneumoniae infection as a risk factor for coronary heart disease in the Helsinki Heart Study. *Ann Intern Med* 116:273-278.
28. Chen, S., R. Sorrentino, K. Shimada, Y. Bulut, T. M. Doherty, T. R. Crother, and M. Arditi. 2008. Chlamydia pneumoniae-induced foam cell formation requires MyD88-dependent and -independent signaling and is reciprocally modulated by liver X receptor activation. *J Immunol* 181:7186-7193.
29. Naiki, Y., R. Sorrentino, M. H. Wong, K. S. Michelsen, K. Shimada, S. Chen, A. Yilmaz, A. Slepenkin, N. W. Schroder, T. R. Crother, Y. Bulut, T. M. Doherty, M. Bradley, Z. Shaposhnik, E. M. Peterson, P. Tontonoz, P. K. Shah, and M. Arditi. 2008. TLR/MyD88 and liver X receptor alpha signaling pathways reciprocally control Chlamydia pneumoniae-induced acceleration of atherosclerosis. *J Immunol* 181:7176-7185.
30. Wick, G., H. Perschinka, and Q. Xu. 1999. Autoimmunity and atherosclerosis. *Am Heart J* 138:S444-449.
31. Kol, A., G. K. Sukhova, A. H. Lichtman, and P. Libby. 1998. Chlamydial heat shock protein 60 localizes in human atheroma and regulates macrophage tumor necrosis factor-alpha and matrix metalloproteinase expression. *Circulation* 98:300-307.
32. Belay, T., F. O. Eko, G. A. Ananaba, S. Bowers, T. Moore, D. Lyn, and J. U. Igietseme. 2002. Chemokine and chemokine receptor dynamics during genital chlamydial infection. *Infect Immun* 70:844-850.
33. Fong, I. W., B. Chiu, E. Viira, D. Jang, and J. B. Mahony. 1999. De Novo induction of atherosclerosis by Chlamydia pneumoniae in a rabbit model. *Infect Immun* 67:6048-6055.
34. Muhlestein, J. B., J. L. Anderson, E. H. Hammond, L. Zhao, S. Trehan, E. P. Schwobe, and J. F. Carlquist. 1998. Infection with Chlamydia pneumoniae accelerates the development of atherosclerosis and treatment with azithromycin prevents it in a rabbit model. *Circulation* 97:633-636.

35. Jackson, D. J., J. P. Rakwar, B. Chohan, K. Mandaliya, J. J. Bwayo, J. O. Ndinya-Achola, N. J. Nagelkerke, J. K. Kreiss, and S. Moses. 1997. Urethral infection in a workplace population of East African men: evaluation of strategies for screening and management. *J Infect Dis* 175:833-838.
36. Hu, H., G. N. Pierce, and G. Zhong. 1999. The atherogenic effects of chlamydia are dependent on serum cholesterol and specific to Chlamydia pneumoniae. *J Clin Invest* 103:747-753.
37. Moazed, T. C., L. A. Campbell, M. E. Rosenfeld, J. T. Grayston, and C. C. Kuo. 1999. Chlamydia pneumoniae infection accelerates the progression of atherosclerosis in apolipoprotein E-deficient mice. *J Infect Dis* 180:238-241.
38. Tsukamoto, K., M. Kinoshita, K. Kojima, Y. Mikuni, M. Kudo, M. Mori, M. Fujita, E. Horie, N. Shimazu, and T. Teramoto. 2002. Synergically increased expression of CD36, CLA-1 and CD68, but not of SR-A and LOX-1, with the progression to foam cells from macrophages. *J Atheroscler Thromb* 9:57-64.
39. Boullier, A., D. A. Bird, M. K. Chang, E. A. Dennis, P. Friedman, K. Gillotre-Taylor, S. Horkko, W. Palinski, O. Quehenberger, P. Shaw, D. Steinberg, V. Terpstra, and J. L. Witztum. 2001. Scavenger receptors, oxidized LDL, and atherosclerosis. *Ann N Y Acad Sci* 947:214-222; discussion 222-213.
40. Faure, E., L. Thomas, H. Xu, A. Medvedev, O. Equils, and M. Arditi. 2001. Bacterial lipopolysaccharide and IFN-gamma induce Toll-like receptor 2 and Toll-like receptor 4 expression in human endothelial cells: role of NF-kappa B activation. *J Immunol* 166:2018-2024.
41. Sakurai, K., and T. Sawamura. 2003. Stress and vascular responses: endothelial dysfunction via lectin-like oxidized low-density lipoprotein receptor-1: close relationships with oxidative stress. *J Pharmacol Sci* 91:182-186.
42. Cominacini, L., A. F. Pasini, U. Garbin, A. Davoli, M. L. Tosetti, M. Campagnola, A. Rigoni, A. M. Pastorino, V. Lo Cascio, and T. Sawamura. 2000. Oxidized low density lipoprotein (ox-LDL) binding to ox-LDL receptor-1 in endothelial cells induces the activation of NF-kappaB through an increased production of intracellular reactive oxygen species. *J Biol Chem* 275:12633-12638.
43. Cominacini, L., A. Rigoni, A. F. Pasini, U. Garbin, A. Davoli, M. Campagnola, A. M. Pastorino, V. Lo Cascio, and T. Sawamura. 2001. The binding of oxidized low density lipoprotein (ox-LDL) to ox-LDL receptor-1 reduces the intracellular concentration of nitric oxide in endothelial cells through an increased production of superoxide. *J Biol Chem* 276:13750-13755.
44. Li, D. Y., H. J. Chen, and J. L. Mehta. 2001. Statins inhibit

oxidized-LDL-mediated LOX-1 expression, uptake of oxidized-LDL and reduction in PKB phosphorylation. *Cardiovasc Res* 52:130-135.

45. Vergnani, L., S. Hatrik, F. Ricci, A. Passaro, N. Manzoli, G. Zuliani, V. Brovkovych, R. Fellin, and T. Malinski. 2000. Effect of native and oxidized low-density lipoprotein on endothelial nitric oxide and superoxide production : key role of L-arginine availability. *Circulation* 101:1261-1266.
46. Nagase, M., K. Ando, T. Nagase, S. Kaname, T. Sawamura, and T. Fujita. 2001. Redox-sensitive regulation of lox-1 gene expression in vascular endothelium. *Biochem Biophys Res Commun* 281:720-725.
47. Li, L., T. Sawamura, and G. Renier. 2004. Glucose enhances human macrophage LOX-1 expression: role for LOX-1 in glucose-induced macrophage foam cell formation. *Circ Res* 94:892-901.

Figure Legends

FIGURE 1. GroEL1 protein induces atherosclerotic lesion formation in HC diet-fed rabbits. A, Representative photographs of atherosclerotic lesions (fatty streak) of aortas stained with Sudan IV. The graph indicates the extent of atherosclerotic lesions in aortas from the 5 experimental groups. Results are expressed as mean ± SEM. *P < 0.05. B, Histopathological features of cross-sections of abdominal aortas were stained using hematoxylin and eosin. The lumen is uppermost in all sections and the internal elastic laminae are indicated with arrows. C and D, Immunohistochemistry to assess infiltrated monocytic cells, LOX-1, SREC, and SR-B1 in rabbit abdominal aortas. Corresponding hematoxylin staining was used for nucleus identification.

FIGURE 2. GroEL1 protein induces LOX-1 expression and enhances oxLDL uptake in HCAECs. A, Intracellular DiI-oxLDL was observed using confocal microscopy. B, Expression of LOX-1, SREC, and SR-B1 mRNA were measured by real-time PCR. Data represent the results of 3 independent experiments (mean ± SEM). *P < 0.05 compared with the unstimulated group. C, Expression of LOX-1, SREC and SR-B1 in HCAECs was detected by immunofluorescence and observed by confocal microscopy. DAPI was used to stain the HCAEC nuclei. D, Membrane and total LOX-1, SREC or SR-B1 protein levels were analyzed with Western blotting. β-actin and Gαs were used as loading controls. The values represent quantification of the proteins expression (fold of control) in HCAECs.

FIGURE 3. GroEL1-induced LOX-1 expression in HCAECs is mediated by TLR4. A, TLR4 and TLR2 protein expression were analyzed. B, HCAECs were pretreated with anti-hTLR4 antibody or transfected with TLR4 siRNA prior to GroEL1 treatment.

LOX-1 mRNA expression was analyzed by real-time PCR. C, HCAECs were pretreated with anti-hTLR2 antibody or transfected with TLR2 siRNA prior to GroEL1 treatment. LOX-1 mRNA expression was analyzed by real-time PCR. Data represent the results of 3 independent experiments (mean ± SEM). *$P < 0.05$.

FIGURE 4. GroEL1 protein upregulates LOX-1 expression in HCAECs by modulating PI3K/Akt-, eNOS-, and p38 MAPK-related mechanisms. A, HCAECs were treated for 6 h with 25–100 μg/mL of GroEL1 protein and Akt activation (phosphorylation) was analyzed by western blot analysis. B, HCAECs were treated for 8 h with 25–100 μg/mL of GroEL1 protein or 5 μM LY294002 (LY) and eNOS phosphorylation and production were analyzed. C, HCAECs were pretreated with 10 μM SB203580 (SB), SP600125 (SP), or PD98059 (PD) for 1 h prior to stimulation with GroEL1 protein for 12 h. D, LOX-1 mRNA expression was analyzed after 12 h of culture in control or GroEL1 protein in the absence or presence of SNOC (100 μM)-containing, L-NAME (10 μM)-containing, or LY294002 (10 μM)-containing medium. Data represent the results of 3 independent experiments (mean ± SEM). *$P < 0.05$. E, LOX-1 protein expression was observed using confocal microscopy after 24 h of culture in control or GroEL1 protein in the absence or presence of SNOC-containing, L-NAME-containing, or LY294002-containing medium.

FIGURE 5. NADPH–oxidase-mediated ROS generation and MAPK signaling pathways are involved in LOX-1 expression. A, NADPH oxidase activity was measured with a superoxide-dependent lucigenin chemiluminescent assay. B, HCAECs were treated with GroEL1 protein. Cytosolic Rac1 activity was measured using a pull-down assay. C, HCAECs were pretreated with PEG-SOD, apocynin

(APO), or DPI or were transfected with 25 nM Rac1 siRNA followed by GroEL1 protein stimulation for 12 h. LOX-1 mRNA expression levels were analyzed by quantitative real-time PCR. H_2O_2 was used as the positive control. Silencer-validated siRNA (NC siRNA) was used for knockdown validation. D, HCAECs were treated with GroEL1 in the presence or absence of 100 μM DPI before the cell lysates were extracted. Phosphorylation of p38 MAPK, ERK1/2, and SAPK/JNK was analyzed by western blotting. E, HCAECs were pretreated with 10 μM SB203580, PD98059, or SP600125 for 1 h before treatment with 100 ng/mL of GroEL1 protein. LOX-1 mRNA levels were evaluated by quantitative real-time PCR. Data represent the results of 3 independent experiments (mean ± SEM; $*P < 0.05$).

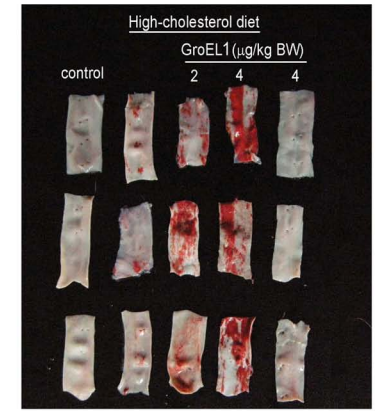
A
High-cholesterol diet
GroEL1(μg/kg BW)
control
2
4
4

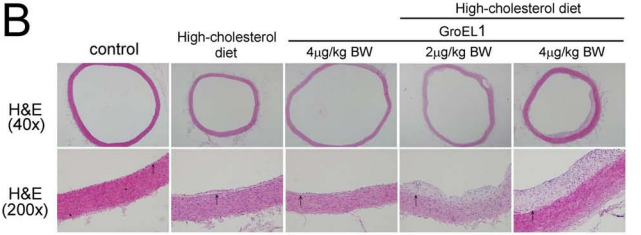
B
High-cholesterol diet
GroEL1
control
High-cholesterol diet
4μg/kg BW
2μg/kg BW
4μg/kg BW
H&E (40x)
H&E (200x)

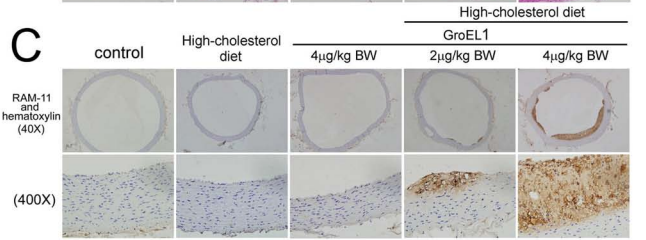
C
High-cholesterol diet
GroEL1
control
High-cholesterol diet
4μg/kg BW
2μg/kg BW
4μg/kg BW
RAM-11 and hematoxylin (40X)
(400X)

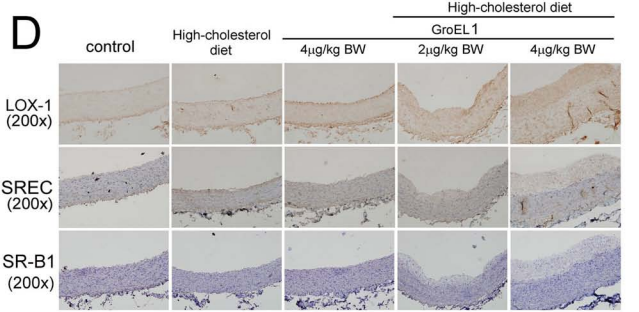
D
High-cholesterol diet
GroEL1
control
High-cholesterol diet
4μg/kg BW
2μg/kg BW
4μg/kg BW
LOX-1 (200x)
SREC (200x)
SR-B1 (200x)

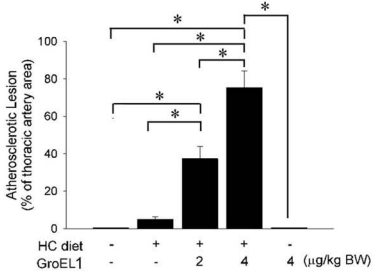
Atherosclerotic Lesion (% of thoracic artery area)
100
80
60
40
20
0
*
HC diet - + + + -
GroEL1 - - 2 4 4 (μg/kg BW)

(Figure 1)

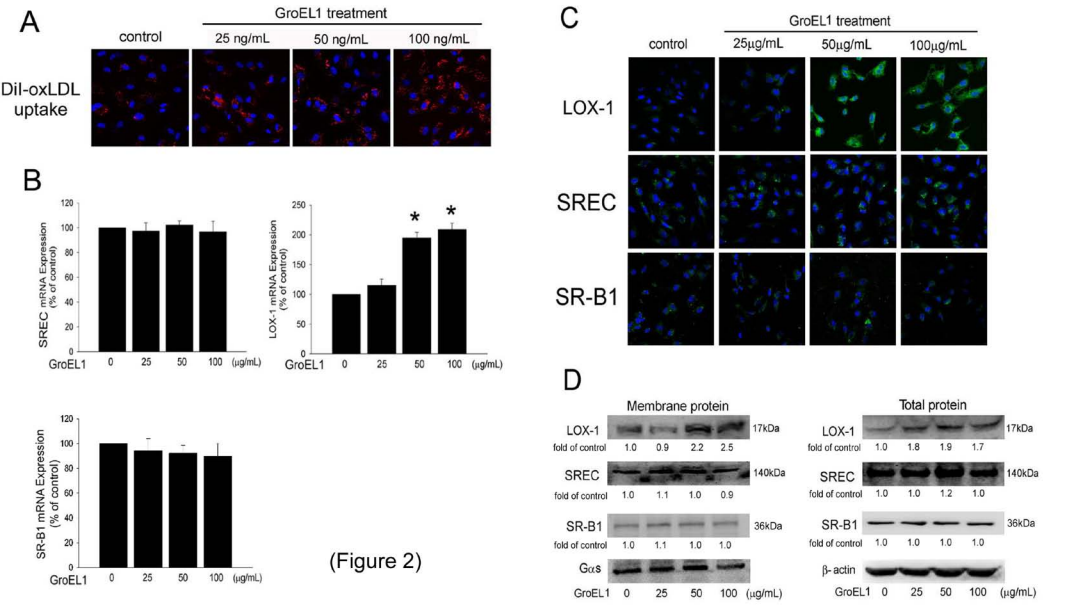
A
GroEL1 treatment
control
25 ng/mL
50 ng/mL
100 ng/mL
DiI-oxLDL uptake
B
SREC mRNA Expression (% of control)
LOX-1 mRNA Expression (% of control)
SR-B1 mRNA Expression (% of control)
GroEL1 0 25 50 100 (μg/mL)
C
GroEL1 treatment
control
25μg/mL
50μg/mL
100μg/mL
LOX-1
SREC
SR-B1
D
Membrane protein
Total protein
LOX-1
SREC
SR-B1
Gαs
β-actin
17kDa
140kDa
36kDa
fold of control
LOX-1 1.0 0.9 2.2 2.5
SREC 1.0 1.1 1.0 0.9
SR-B1 1.0 1.1 1.0 1.0
LOX-1 1.0 1.8 1.9 1.7
SREC 1.0 1.0 1.2 1.0
SR-B1 1.0 1.0 1.0 1.0
GroEL1 0 25 50 100 (μg/mL)

(Figure 2)

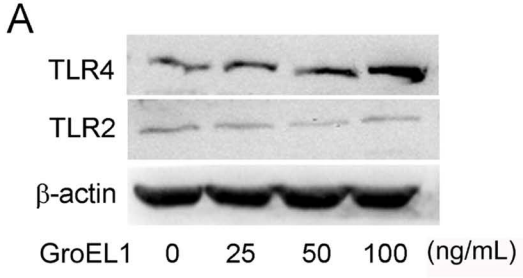
A
TLR4
TLR2
β-actin
GroEL1 0 25 50 100 (ng/mL)

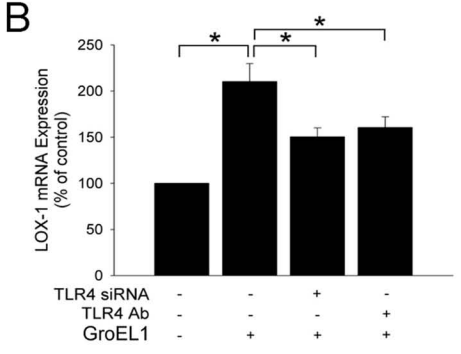
B
LOX-1 mRNA Expression (% of control)
250
200
150
100
50
0
*
*
*
TLR4 siRNA - - + -
TLR4 Ab - - - +
GroEL1 - + + +

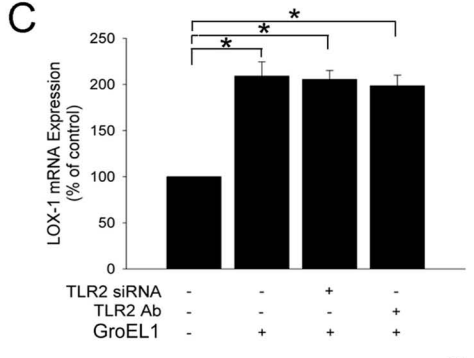
C
LOX-1 mRNA Expression (% of control)
250
200
150
100
50
0
*
*
*
TLR2 siRNA - - + -
TLR2 Ab - - - +
GroEL1 - + + +

(figure 3)

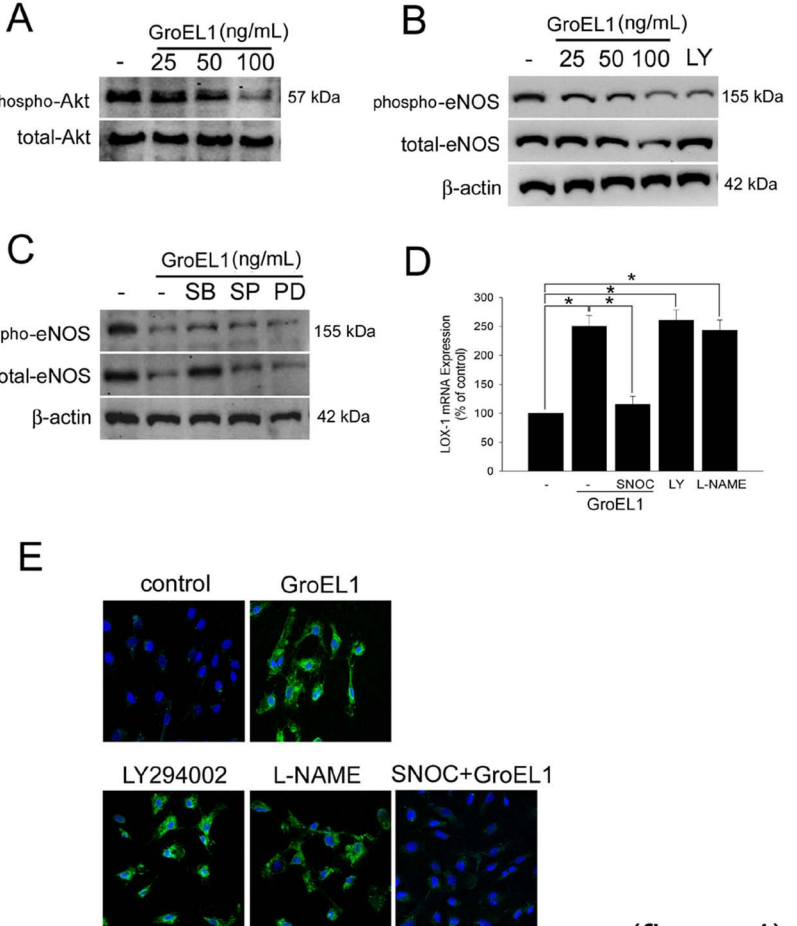
A
GroEL1 (ng/mL)
- 25 50 100
phospho-Akt
total-Akt
57 kDa
B
GroEL1 (ng/mL)
- 25 50 100 LY
phospho-eNOS
total-eNOS
β-actin
155 kDa
42 kDa
C
GroEL1 (ng/mL)
- - SB SP PD
phospho-eNOS
total-eNOS
β-actin
155 kDa
42 kDa
D
LOX-1 mRNA Expression (% of control)
300
250
200
150
100
50
0
- - SNOC LY L-NAME
GroEL1
E
control
GroEL1
LY294002
L-NAME
SNOC+GroEL1

(figure 4)

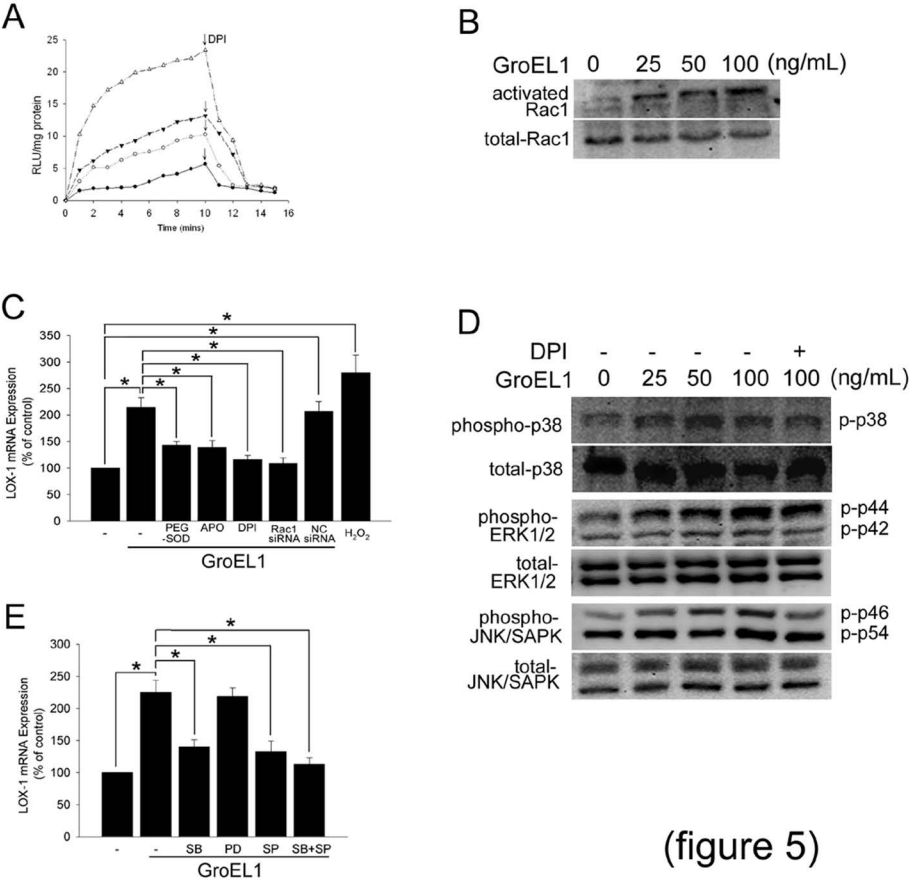
A
DPI
RLU/mg protein
Time (mins)
B
GroEL1 0 25 50 100 (ng/mL)
activated Rac1
total-Rac1
C
LOX-1 mRNA Expression (% of control)
PEG -SOD
APO
DPI
Rac1 siRNA
NC siRNA
H2O2
GroEL1
D
DPI - - - - +
GroEL1 0 25 50 100 100 (ng/mL)
phospho-p38
total-p38
p-p38
phospho-ERK1/2
total-ERK1/2
p-p44
p-p42
phospho-JNK/SAPK
total-JNK/SAPK
p-p46
p-p54
E
LOX-1 mRNA Expression (% of control)
SB
PD
SP
SB+SP
GroEL1

(figure 5)